Communication

Porous BCN Nanotubular Fibers: Growth and Spatially Resolved Cathodoluminescence

Long-Wei Yin, Yoshio Bando, Dmitri Golberg, Alexandre Gloter, Mu-Sen Li, Xiaoli Yuan, and Takashi Sekiguchi

J. Am. Chem. Soc., **2005**, 127 (47), 16354-16355• DOI: 10.1021/ja054887g • Publication Date (Web): 26 October 2005

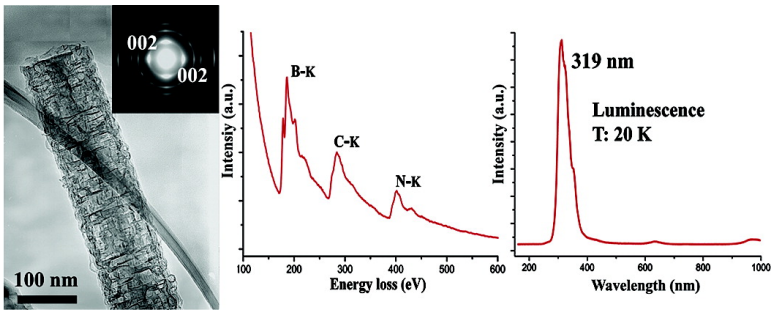

More About This Article

Additional resources and features associated with this article are available within the HTML version:

- Supporting Information
- Links to the 5 articles that cite this article, as of the time of this article download
- Access to high resolution figures
- Links to articles and content related to this article
- Copyright permission to reproduce figures and/or text from this article

View the Full Text HTML

J|A|C|S
COMMUNICATIONS

Published on Web 10/26/2005

Porous BCN Nanotubular Fibers: Growth and Spatially Resolved Cathodoluminescence

Long-Wei Yin,*[,†,‡] Yoshio Bando,[†,§] Dmitri Golberg,[†,§] Alexandre Gloter,[¶] Mu-Sen Li,[‡] Xiaoli Yuan,[§] and Takashi Sekiguchi[§]

Advanced Materials Laboratory, National Institute for Materials Science, Namiki 1-1, Tsukuba, Ibaraki 305-0044, Japan, School of Materials Science and Engineering, Shandong University, Jinan 250061, China, Nanomaterials Laboratory, National Institute for Materials Science, Namiki 1-1, Tsukuba, Ibaraki 305-0044, Japan, and University Paris-Sud 11, CNRS, UMR 8502, Orsay F-91405, France

Received July 21, 2005; E-mail: yin.longwei@nims.go.jp

Recently, significant research interest has been shifted from C-based toward BN-based nanostructures. The latter are most commonly represented by hexagonal BN nanotubes possessing stable insulating properties (~5.5 eV band gap).[1] Ternary B−C−N materials are attractive semiconductors with a "tunable" band gap energy that is primarily controlled by the structure chemical composition.[2] Experimental evidences of BC_xN compound formation with x of 2.5,[3a] 3,[3b] or 4[3c] have been presented. As one of the important B−C−N materials, BC_2N nanotubes have been intensively studied theoretically[4a] and experimentally.[4b,c]

A homogeneously structured $B_xC_yN_z$ nanotube represents a novel layered system that may be a hybrid of hexagonal boron nitride and graphite. This material should exhibit semiconducting properties and may find applications as lightweight electrical conductors, current rectifiers, transistors, light emission diodes, and lasers. Recently, transport measurements performed on individual bundles of homogeneously structured BC_xN nanotubes have confirmed their natural semiconductor character.[5] Despite several studies related to the synthesis and analysis of $B_xC_yN_z$ nanotubes, the clear relationship between structure, band gap, and optical properties has not yet been understood. For example, BC_2N nanotubes were quoted to possess different band gaps, 2.1 eV[6a] or 1.4 eV,[6b] when different examination methods were in use. A band gap of 1.0 eV for $B_{0.34}C_{0.42}N_{0.24}$ nanotube has recently been reported.[6c] It is important to further explore the structure/chemistry dependence of a band gap and resultant optical properties for homogeneous $B_xC_yN_z$ nanotubes in order to promote their successful integration into modern nanoelectronics and nanophotonics.

In this communication, a new type of porous boron carbonitride tubular fibers with homogeneous B, C, and N species distribution corresponding to BCN stoichiometry was synthesized. Optical properties and band gap energy of individual BCN tubular fibers were studied via spatially resolved cathodoluminescence (CL). In parallel, BCN nanotubes were examined using HRTEM, EELS, electron diffraction (ED), and EDS. The spatially resolved CL measurements on individual BCN tubular fibers clearly revealed the characteristics of a semiconductor with a band gap of 3.89 eV.

The BCN tubular fibers were synthesized via chemical vapor deposition (CVD) using as-prepared B−N−O precursors.[7] The B−N−O and graphite powders were mechanically mixed (15:1 mole ratio) and put into a BN crucible. The precursors were heated at 1800 °C in a graphite susceptor placed into an induction furnace. To synthesize BCN materials with homogeneous B, C, and N distribution, CH_4 gas was introduced into the system carried by an Ar gas flow (Ar/CH_4 gas flow rate: 30:1) from the bottom of the furnace, while a NH_3 flow was set from the top of the furnace. A B_2O_3 vapor from the B−N−O decomposition together with methane reacted with ammonia to form BCN tubular fibers, which deposited on the graphite susceptor walls at 1200 °C. The synthesis was run over 2 h.

The yield of the BCN tubular fibers was measured to be ~45% with respect to the starting material mass. The resultant tubular fibers were analyzed using 300 kV field emission high-resolution transmission electron microscopes (JEOL-3000F and JEOL-3100FEF) equipped with a Gatan-766 EEL spectrometer and in-column Omega Filter, respectively. Figure 1a illustrates a tubular structure observed within a synthesized product. There were no metal particles at the fiber tip ends; the tubes were typically open. The fibers have uniform diameters in the range of 100−140 nm and a length of up to 10 μm. The inset in Figure 1a is a typical ED pattern taken from an individual fiber. The well-defined crystalline feature of the ED pattern is the intense rows of (002), (004), etc. reflections either perpendicular or parallel to the fiber axis, implying that the (002) BCN graphitic planes are preferentially either parallel or perpendicular to the growth axis, thus creating novel porous, fractal-like wall structure of a tube. This is a new type of BCN structure, quite different from the previously reported BN,[1] BC_xN,[2−6] and fluorinated BN[8a] nanostructures. In fact, HRTEM image (Figure 1b) clearly demonstrates that the tube walls are composed of highly crystalline BCN fragments organized in a fractal fashion and leading to a porous-like appearance of the walls. EELS taken from an individual tubular fiber (Figure 1c) shows that the nanostructure is composed of B, C, and N. The analysis from the K-edge absorption for B, C, and N shows that the overall chemical composition of the tubular fibers is commensurate with the BCN stoichiometry. Elemental maps collected from an individual fiber (Figure 2) reveal that all constituting B, C, and N elements are homogeneously distributed in the nanostructure (within a spatial resolution of the energy-filtering images of ~5 Å). The resulting surface area of the BCN nanotubular fibers determined by the BET[8b] adsorption isotherms was measured to be 427 m^2/g, which is relatively higher than that of BN nanotubes (254 m^2/g)[8c] and activated BN (168 m^2/g).[8d]

Spatially resolved CL measurements and in situ CL imaging on individual tubular fibers were then performed. The samples were first deposited on a standard copper TEM grid and thoroughly characterized using TEM. CL spectra from an individual BCN nanotube were obtained with a high-resolution CL system performing at an accelerating voltage of 5 kV and a current of 1.2 nA in a low-energy CL system inside a thermal field emission electron microscope (TFE-SEM, Hitachi S4200).

Figure 3b depicts a CL spectrum taken from an individual BCN tubular fiber (Figure 3a) at 300 K. The CL emission at 300 K is rather weak. The spectrum is basically composed of a relatively

† Advanced Materials Laboratory, National Institute for Materials Science.
‡ Shandong University.
§ Nanomaterials Laboratory, National Institute for Materials Science.
¶ University Paris-Sud.

10.1021/ja054887g CCC: $30.25

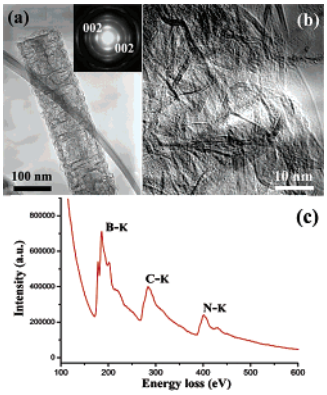

Figure 1. (a) Low-magnification TEM image of a porous BCN tubular fiber; the inset in (a) is its ED pattern. (b) High-magnification TEM image. (c) EEL spectrum taken from the nanotubular fiber corresponding to the B/C/N ∼ 1:1:1 atomic ratios.

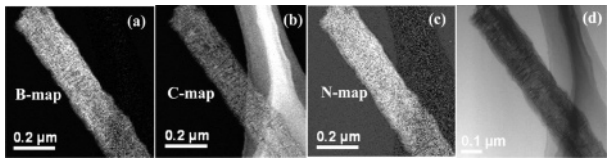

Figure 2. (a−c) Spatially resolved elemental EELS maps implying the uniform distribution of the B, C, and N species within a nanostructure and (d) corresponding zero-loss image of the BCN nanotubular fiber.

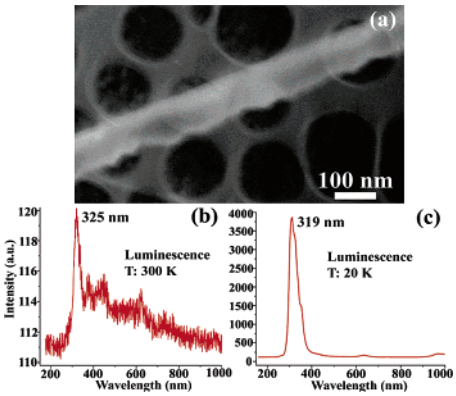

Figure 3. A SEM image of an individual porous BCN tubular fiber on a copper grid (a) and CL spectra (a) at 300 K (b) and 20 K (c), respectively.

sharp emission peak at 325 nm and several weaker emissions centered at 390, 470, and 610 nm associated with insurmountable structural defects. Figure 3c displays a CL spectrum taken at 20 K from the same sample. The emission peak shifts from 325 nm (at 300 K) to 319 nm (at 20 K). Furthermore, the 319 nm emission peak at 20 K becomes notably sharper and intense. Figure 4a shows CL spectra taken from another fiber (stretching across a large hole of a copper TEM grid) at 20 K. The CL spectra denoted as 1, 2, 3, and 4 were taken from different spots within or around the sample (Figure 4b). Sharp and intense ultraviolet emission centered at 319 nm at 20 K is visible (Figure 4c). More than several tens of individual fibers have been characterized via CL, and the results were reproducible. The above-mentioned structural characterization has shown the homogeneous B, C, and N species distributions with overall BCN stoichiometry, thus the possibility that the dominant CL emission peak derives from pure *h*-BN or graphitic carbon can be excluded. Therefore, it is clearly indicated that the present cathodoluminescence is indeed derived from individual BCN tubular fibers. It is logically assumed that the sharp CL ultraviolet emission centered at 319 nm is the band-edge luminescence, suggesting the band gap energy of ∼3.89 eV for the present porous BCN tubular

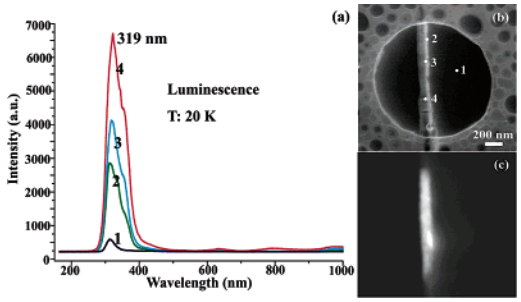

Figure 4. (a) CL spectra recorded at 20 K from various spots along an individual porous BCN tubular fiber in (b). The fiber reveals a band gap energy of 3.89 eV. (c) CL luminescence image from the fiber inside TFE-SEM.

material. The CL ultraviolet emission from the samples was very stable during the entire measurements. The band gap energy of the nanomaterial obtained via CL examinations is wider than those reported for BC_2N[6a,b] and $B_{0.34}C_{0.42}N_{0.24}$[6c] nanotubes. So it is suggested to be particularly advantageous for ultimate ultraviolet optical applications.

In summary, a new type of porous boron carbonitride nanotubular fibers with the overall BCN stoichiometry and homogeneous B, C, and N species distributions was fabricated via the CVD method. Spatially resolved CL measurements and in situ CL imaging for individual nanostructures were carried out. CL spectra clearly revealed intense ultraviolet emission centered at 319 nm, suggesting the characteristics of a semiconductor with a band gap of 3.89 eV. It is believed that the material may find a variety of applications in ultraviolet optical devices, gas storage systems, and field emission apparatus.

Acknowledgment. This work was partially supported by Program for New Century Excellent Talents in University (NCET).

Supporting Information Available: Preparation and formation (S1); SEM image (S2); EELS and EDX spectra (S3); TEM image (S4); ED pattern (S5); HRTEM image (S6), and full citation of ref 5 (S7) (PDF). This material is available free of charge via the Internet at http://pubs.acs.org.

References

(1) (a) Chopra, N. G.; Luyken, R. J.; Cherrey, K.; Crespi, V. H.; Cohen, M. L.; Louie, S. G.; Zettl, A. *Science* **1995**, *269*, 966. (b) Blase, X.; Rubio, A.; Louie, S. G.; Cohen, M. L. *Europhys. Lett.* **1994**, *28*, 335. (c) Han, W. Q.; Zettl, A. *Appl. Phys. Lett.* **2002**, *81*, 5051. (d) Han, W. Q.; Zettl, A. *J. Am. Chem. Soc.* **2003**, *125*, 2062. (e) Wu, J.; Han, W. Q.; Walukiewicz, W.; Ager, J. W., III; Shan, W.; Haller, E. E.; Zettl, A. *Nano Lett.* **2004**, *4*, 647.

(2) (a) Golberg, D.; Bando, Y.; Dorozhikin, P.; Dong, Z. C. *MRS Bull.* **2004**, *29*, 38. (b) Bai, X. D.; Wang, E. G.; Yu, J.; Yang, H. *Appl. Phys. Lett.* **2000**, *77*, 67. (c) Bai, X. D.; Guo, J. D.; Yu, J.; Wang, E. G.; Yuan, J.; Wang, W. *Appl. Phys. Lett.* **2000**, *76*, 2624.

(3) (a) Maya, L. *J. Am. Ceram. Soc.* **1988**, *71*, 1104. (b) Kawaguchi, M.; Kawashima, T. *J. Chem. Soc. Chem. Commun.* **1993**, (14) 1133. (c) Bill, J.; Riedel, R. *Mater. Res. Symp. Proc.* **1992**, *271*, 839.

(4) (a) Miyamoto, Y.; Rubio, A.; Cohen, M. L.; Louie, S. G. *Phys. Rev. B* **1994**, *50*, 4976. (b) Weng-Sieh, Z.; Cherrey, K.; Chopra, N. G.; Blase, S.; Miyamoto, Y.; Rubio, A.; Cohen, M. L.; Louie, S. G.; Zettl, A.; Gronsky, R. *Phys. Rev. B* **1995**, *51*, 11229. (c) Sasaki, T.; Akaishi, M.; Yamaoka, S.; Fujiki, Y.; Oikawa, T. *Chem. Mater.* **1993**, *5*, 695.

(5) Terrones, M. et al. *Adv. Mater.* **2003**, *15*, 1899.

(6) (a) Watanabe, M. O.; Itoh, S.; Sasaki, T.; Mizushima, K. *Phys. Rev. Lett.* **1996**, *77*, 187. (b) Chen, Y.; Barnard, J. C.; Palmer, R. E.; Watanabe, M. O.; Sasaki, T. *Phys. Rev. Lett.* **1999**, *83*, 2406. (c) Yu, J.; Ahn, J.; Yoon, S. F.; Zhang, Q.; Gan, R. B.; Chew, K.; Yu, M. B.; Bai, X. D.; Wang, E. G. *Appl. Phys. Lett.* **2000**, *77*, 1949.

(7) (a) Ma, R.; Bando, Y.; Sato, T. *Adv. Mater.* **2002**, *14*, 366. (b) Zhu, Y. C.; Bando, Y.; Xue, D. F.; Sekiguchi, T.; Golberg, D.; Xu, F. F.; Liu, Q. L. *J. Phys. Chem. B* **2004**, *108*, 6193.

(8) (a) Tang, C. C.; Bando, Y.; Huang, Y.; Yue, S. L.; Gu, C. Z.; Xu, F. F.; Golberg, D. *J. Am. Chem. Soc.* **2005**, *127*, 6552. (b) Brunauer, S.; Emmett, P. H.; Teller, E. *J. Am. Chem. Soc.* **1938**, *60*, 309. (c) Tang, C. C.; Bando, Y.; Ding, X.; Qi, S.; Golberg, D. *J. Am. Chem. Soc.* **2002**, *124*, 14550. (d) Han, W. Q.; Brutchey, R.; Tilley, T. D.; Zettl, A. *Nano Lett.* **2004**, *4*, 173.

JA054887G